4 Channel response to flood diversion into floodplains

Lateral diversion structures in rivers are common measures used to divert parts of the discharge during flood events. The lateral overflow reduces discharge and thus bedload transport capacity in the main channel, resulting in sediment deposition. In this chapter, interactions between lateral discharge and changes in bed level are discussed and illustrated using 1D and 2D modelling approaches, and recommendations for practical model applications are provided. Further, aspects of ecological flooding of retention areas are briefly discussed.

Seline Frei, Eva Gerke, Robert Boes and David Vetsch

4.1 Introduction

Lateral diversion structures in rivers, such as side weirs (lateral weirs) and overflow embankments, are common measures used to divert part of the discharge into a lateral retention area or into a flood corridor during major flood events. In this way, the inundation risk for downstream areas can be reduced. While both regulated and unregulated lateral diversion structures exist, most of them are unregulated in Switzerland (Bühlmann and Boes 2014).

Lateral overflow occurs as soon as the water level reaches the dam or weir crest. The crest height has to be designed according to hydrological and flood protection goals, and in Switzerland the protection objective is based on a risk assessment and determined based on the damage potential of the flood-prone area (FOEN 2005). The design overflow discharge is therefore a project-specific value. Lateral diversion structures are used in flood protection, both as part of the design concept and for system safety during extreme events (overload scenario). Lateral overflow is typically considered upstream from areas with high vulnerability, such as clustered settlements and industrial facilities, provided that appropriate retention areas are available or flood corridors can be used to convey the lateral overflow. Lateral overflow leads to discharge reduction and thus lower bedload transport capacity in the main channel. Consequently, local deposition near the lateral diversion structure and sediment aggradation in the downstream channel may occur (Fig. 22). The bed level increase may enlarge the lateral overflow considerably compared with a situation without bedload.

As the duration of the flood increases, the aggradation continues to expand towards the downstream main channel. During the falling limb of the flood wave, erosion occurs again where local deposition and sediment aggradation had occurred. However, the interaction between lateral overflow and changes in bedload dynamics in the river must not be neglected in the design of lateral diversion structures. Design guidelines for lateral diversion structures that do not consider sediment aggradation can be found in Bühlmann and Boes (2014), Giesecke *et al.* (2014) and Jäggi *et al.* (2015). To account for the effect of bed level increase on lateral overflow, Rosier (2007) conducted several flume experiments at the Platform PL-LCH at EPFL.

Figure 22

Lateral diversion structure with local bedload deposition and sediment aggradation due to lateral overflow during a flood event. Figure adapted from Rosier (2007).

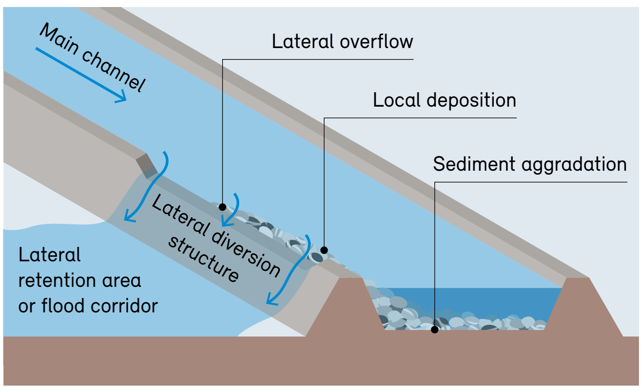

Source: VAW, ETH Zurich

Numerical models commonly used in hydraulic engineering and for flood risk assessment, i.e. 1D and 2D models based on shallow-water equations, can be used as tools for the design of lateral diversion structures considering bed level changes. The simulation software BASEMENT (Vetsch *et al.* 2020) has been applied to analyse the interaction between lateral overflow and changes in bed level, using findings from flume experiments (Rosier 2007) to validate the results. In this chapter model capabilities and requirements are shown and recommendations are provided.

Another aspect that is rather novel in Switzerland is the use of lateral overflow to improve ecological conditions in retention areas in what has been termed 'ecological flooding' (see Box 7). In such a system, water is diverted into the retention areas not only during major but also during minor flood events. This may support the formation of dynamic floodplain biotopes. In Germany, ecological flooding has been successfully employed, for example at the Altenheim polder along the Rhine river, which has existed since 1987 (Pfarr *et al.* 2014).

4.2 Estimation of lateral overflow

4.2.1 Common approaches

Classical weir equations for discharge estimation assume that the flow approaches the weir perpendicular to the weir axis. In contrast, the flow approaches lateral diversion structures at an angle of <90°. Figure 23 shows the top and side views of a lateral diversion structure in a channel with subcritical flow conditions where the flow is diverted towards a lateral retention area or a flood corridor. All variables described below are depicted in Figure 23.

The water depth along the lateral diversion structure is increasing for subcritical (flow velocity < wave speed; Fig. 23b) and decreasing for supercritical (flow velocity > wave speed) conditions. Therefore, the lateral unit overflow for supercritical flow is distinctly smaller than for subcritical flow and almost impossible to predict (Jäggi *et al.* 2015). Lateral diversion structures are not recommended for supercritical flow (Hager 2010) and thus should only be considered in subcritical river reaches with an upstream Froude number $Fr_o = v_o/(g \cdot A/B_w)^{0.5} < 0.75$ (Hager 2010; Giesecke *et al.* 2014), where $v_o = Q_o/A$ = velocity of the approaching flow averaged over the cross-section, Q_o = upstream discharge, A = cross-sectional flow area, g = acceleration of gravity, and B_w = top width of the water surface. Several approaches for estimating the lateral overflow Q_D are available in the literature, and they are commonly based on the assumption of no energy loss over the lateral diversion structure.

For the calculation of lateral overflow in a rectangular, horizontal channel with a lateral sharp crested weir, De Marchi (1934) proposed the equation:

$$\frac{dQ_D}{dx} = \frac{2}{3} \cdot C_M \cdot \sqrt{2g} \cdot (h_W - w)^{2/3} \qquad (1)$$

$\frac{dQ_D}{dx}$ rate of change in discharge along the lateral diversion structure [m³ (m⁻¹ s⁻¹)]

Figure 23

(a) Top view and (b) side view of a lateral diversion structure, showing the water profile under subcritical channel flow conditions. All variables are defined in the main text. Figure adapted from Bollrich 2013.

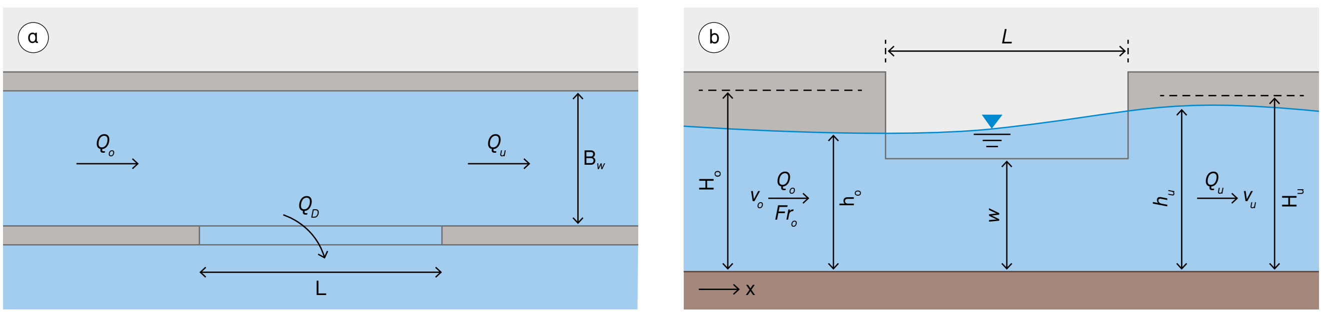

Source: VAW, ETH Zurich

C_M side weir discharge coefficient [-]

Q_D lateral overflow [m^3 s^{-1}]

$h_W = h_W(x)$ water depth along the lateral diversion structure [m]

w lateral diversion structure crest height [m]

g acceleration of gravity [m s^{-2}]

De Marchi's approach is based on the solution to a 1D dynamic equation for gradually varied flow with non-uniform discharge and non-constant water depth $h_W(x)$ along the structure (Di Bacco and Scorzini 2019). For lateral sharp-crested weirs in rectangular and trapezoidal channels under subcritical conditions, the discharge coefficient C_M can be determined according to the simplified approach of Hager (1987) (Eq. 2). There is little literature on side weir discharge coefficients for broad-crested (e.g. Ranga Raju 1979), round-crested (e.g. Izadinia and Heidarpour 2016) or roof-shaped lateral diversion structures. The side weir discharge coefficient strongly influences the calculated lateral overflow. Here, the De Marchi approach with C_M defined by Hager (1987) is used:

$$C_M = 0.728\sqrt{\frac{2+Fr_o^2}{2+3Fr_o^2}} \quad (2)$$

For many situations, the upstream discharge Q_o, the downstream discharge Q_u, and the flow conditions in the downstream channel (downstream velocity v_u, water depth h_u, hydraulic head H_u and channel width B) can be defined. Assuming no energy loss along the lateral diversion structure, the upstream flow conditions (upstream velocity v_o, water depth h_o and hydraulic head H_o) can be calculated using the Bernoulli equation. Di Bacco and Scorzini (2019) proposed the following equation to calculate the necessary length of the lateral diversion structure L to reduce Q_o to Q_u:

$$L = \frac{3B}{2C_M}\cdot(\Phi_u - \Phi_o) \quad (3)$$

where $\Phi_i = \frac{2H_i-3w}{H_i-w}\cdot\sqrt{\frac{H_i-h_i}{h_i-w}} - 3\cdot arcsin\left(\frac{H_i-h_i}{h_i-w}\right)$ and $i = o,u$

4.2.2 Impact of morphodynamics

Lateral overflow during a flood event reduces the bedload transport capacity in the main channel. Thus, local deposition near the lateral diversion structure and sediment aggradation in the main channel downstream of the lateral diversion structure may occur (Fig. 22). The local deposition starts at the beginning of the lateral diversion structure (weir) and reaches its maximum height at the downstream end of the weir. The lateral overflow might increase by a factor of up to three due to the sediment aggradation (Rosier 2007).

Rosier (2007) presented an empirical and iterative way to estimate the local deposition due to a lateral diversion structure based on physical experiments (see also Rosier *et al.* 2008). The iterative estimation is cumbersome and requires the setup of a numerical model and hydrodynamic simulation for each iteration step. However, a detailed estimation of the sediment aggradation and lateral overflow using numerical model simulations, including bedload transport, is recommended for designing lateral diversion structures and is presented here.

4.3 Numerical Modelling of lateral diversion structures

4.3.1 Modelling approaches

To assess the impact of sediment aggradation dynamics on lateral overflow, different numerical modelling approaches were evaluated using the software BASEMENT version 2.8.2, a freeware for simulating river hydro- and morphodynamics (*www.basement.ethz.ch*) developed at the at the VAW of ETH Zurich. Several hydrodynamic (fixed bed, no bedload transport) and morphodynamic simulations were run considering the different modelling approaches, and results were compared with observed experimental data from Rosier (2007). Specifically, trapezoidal and rectangular channels with lateral diversion structures were simulated. Four different numerical modelling approaches were tested, three of which were selected (Fig. 24):

(a) **1D:** The lateral overflow due to a lateral diversion structure is implemented in a 1D BASEMENT model considering the reduction of water with specific sink terms

(Eq. 1) at each cross section along the lateral diversion structure. Specific C_M values must be defined for the specific sink terms. The loss of streamwise momentum due to lateral overflow is considered in BASEMENT.

(b) **1D–2D coupled**: The laterally coupled model in BASEMENT includes a 1D channel and a 2D floodplain. Lateral overflow is computed using Eq. 1, and a specific C_M value must be defined. The reduction of streamwise momentum due to lateral overflow is considered in BASEMENT.

(c) **2D**: The geometry of the lateral diversion structure and the topography of the surrounding overflow section is modelled. C_M does not have to be specified for this simulation.

Examples of these approaches are provided on the BASEMENT website (*www.basement.ethz.ch* > Download > Test cases).

4.3.2 Comparison of different modelling approaches

1D or 1D–2D coupled models are most suitable for straight river reaches. Usually, these models require less topography data and have a short computing time. Neither of these model types shows the flow deviation in the main channel and the floodplain. The 1D–2D coupled model approach may be favourable when the flow field in the floodplain is of importance. Regarding the lateral overflow, the side weir discharge coefficient is the most sensitive parameter and a corresponding sensitivity analysis is recommended. Good results for rectangular channels with a sharp-crested weir and for trapezoidal channels with a roof-shaped weir can be achieved using the side weir discharge coefficient from Hager (1987) (Eq. 2). In Table 3, the 1D and 1D–2D coupled simulations are compared with the 2D simulation, where no C_M value is needed, and with the physical experiment conducted by Rosier (2007).

For the 2D model, the topography must be provided and the roughness at the weir crest has to be specified. However, the lateral overflow is less sensitive to roughness

Figure 24

(a) 1D, (b) 1D–2D coupled, and (c) 2D approaches used in the software BASEMENT to model lateral overflow at a lateral diversion structure.

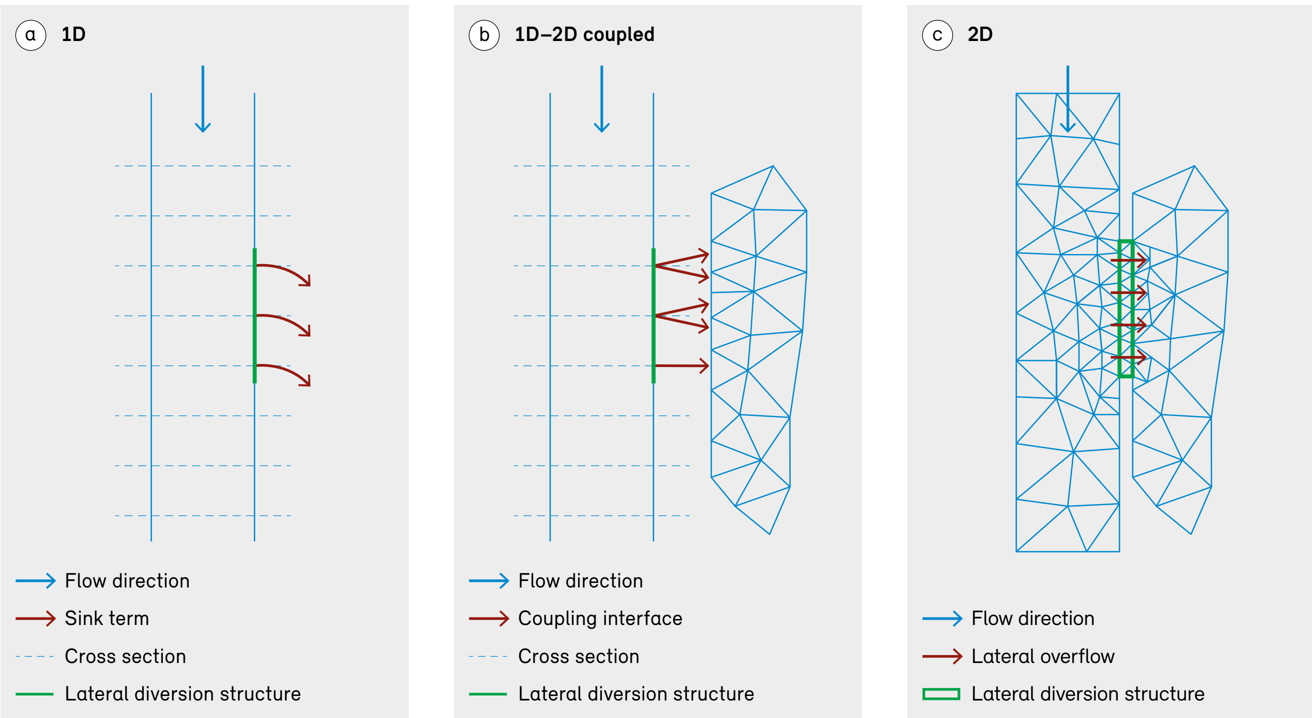

Source: VAW, ETH Zurich

than the 1D or 1D–2D coupled model is to the side weir discharge coefficient. The 2D model gives the flow deviation in the main channel and floodplain.

4.3.3 Impact of morphodynamics

For the design of lateral diversion structures in rivers with distinct bedload transport, morphodynamic simulations are recommended. The sediment aggradation downstream of the lateral diversion structure and the resulting higher lateral overflow can be simulated with all three modelling approaches. However, the spatial extent of the local deposition near the lateral diversion structure cannot be captured with a 1D model. The lateral overflow, sediment aggradation, and geometry and location of the local deposition calculated in the morphodynamic 2D model (Fig. 25) are in good agreement with the physical experiments conducted by Rosier (2007).

Table 3 compares the lateral overflow for the hydro- and morphodynamic simulations, as well as the physical experiment conducted by Rosier (2007). The lateral overflow is significantly greater in the morphodynamic simulations where bedload deposition is considered. In the purely hydrodynamic model, the lateral overflow might be underestimated and the retention area or flood corridor might be designed with insufficient capacity.

Table 3

Comparison of the lateral overflow (Q_D in [l s^{-1}]) between the hydrodynamic and morphodynamic simulations and the physical experiment B02 by Rosier (2007). The rectangular flume has the following dimensions: width = 1.5 m, bottom slope = 0.2%, length of lateral diversion structure L = 3 m, weir height w = 10 cm, constant discharge Q_o = 181 l s^{-1}.

	Hydrodynamic	Morphodynamic	Morphodynamic (with riprap)
Physical experiment by Rosier (2007)	–	52	–
1D model (C_M=0.6 for all 11 sink terms)	33	48	43
1D–2D coupled model (C_M=0.6)	33	47	43
2D model	32	42	40

Figure 25

Local deposition along the lateral diversion structure and sediment aggradation in the main downstream channel (2D model from the B02 experiment from Rosier (2007), lateral diversion structure L = 3 m).

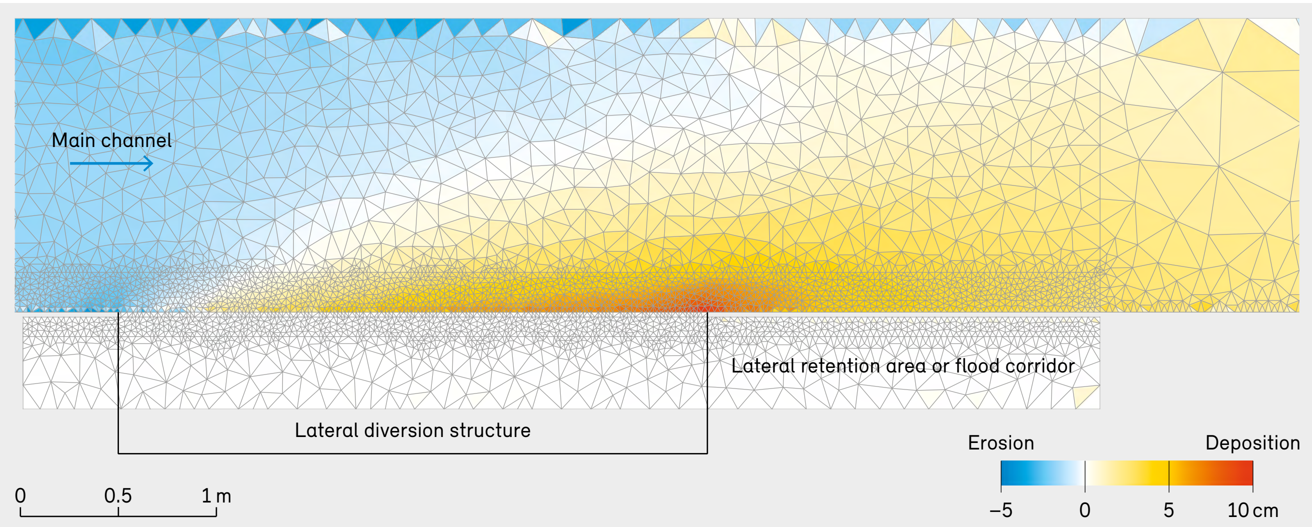

Source: VAW, ETH Zurich.

The water surface elevation and the bed elevation for the hydrodynamic simulation and for the morphodynamic simulations with and without riprap are shown in Figure 26 for the 1D modelling approach. The same results are obtained with the 1D–2D and 2D modelling approaches. A significant amount of sediment can be deposited downstream of the lateral diversion structure and consequently reduce the cross-sectional area (Fig. 26b). There is less water in the channel downstream of the lateral diversion structure, so no rise in water level occurs (Fig. 26). Due to the drawdown curve upstream of the lateral diversion structure (Fig. 26a), stabilization of the bed with riprap is recommended (Tab. 3 and Fig. 26c). The sediment aggradation and local deposition become larger as the length of the lateral diversion structure increases.

Lateral overflow responds rapidly to discharge changes, unlike local deposition and aggradation. The analysis with a short flood hydrograph shows less aggradation, less local deposition and less lateral overflow compared with a simulation with a long flood hydrograph. During the falling limb of the flood hydrograph, the local deposition and the sediment aggradation are completely eroded again and the bed level prior to flooding is restored.

4.3.4 Effect of spatial discretization

The main channel in 1D or 1D–2D coupled models is discretized using cross sections. The water depth, velocity and lateral overflow can be simulated with three to four cross sections along the lateral diversion structure for hydrodynamic simulations. Multiple cross sections (up to 10) along the lateral diversion structure lead to smoother morphodynamic simulation results.

In 2D models, the system is spatially discretized into mesh cells (Figs 24c, 25). Small mesh cells at the lateral diversion structure are necessary to capture the local deposition in morphodynamic simulations. As a rule of thumb, the mesh cells close to the lateral diversion structure should be smaller than *B/20* to capture the local deposition. In hydrodynamic simulations and up- and downstream of the lateral diversion structure, larger mesh cells may be reasonable.

4.4 Recommendations for practical applications

Empirical approaches (e.g. Eq. 1) can be used to roughly estimate lateral overflow, but they are limited to steady flow analysis and do not consider bed level changes in the

Figure 26

Bed elevation and water surface elevation for the 1D modelling approach, for (a) hydrodynamic, (b) morphodynamic, and (c) morphodynamic (with riprap) simulations. The settings of the simulations are described in Table 3.

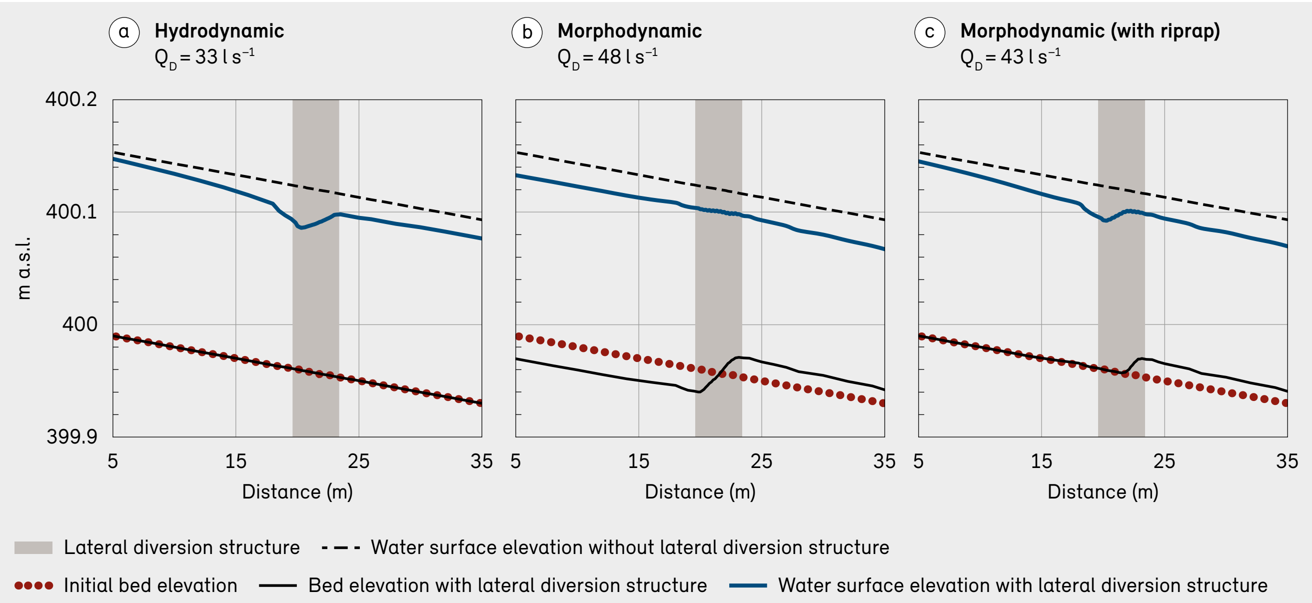

Source: VAW, ETH Zurich

Table 4

Advantages (green) and disadvantages (orange to red) of the three modelling approaches for the simulation of lateral flow diversion.

	1D	**1D–2D coupled**	**2D**
Lateral overflow model	Sink, using Eq. 1	Model coupling, using Eq. 1	Topography of the overflow section
Parameter for lateral overflow	For each cross section with lateral overflow: *Weir crest height* *Weir crest length* C_M	*Weir crest height* C_M	*Roughness* for weir crest
Hydrodynamic results			
Lateral overflow prediction	Good	Good	Good
Flow in channel	No flow diversion[1]	No flow diversion[1]	Flow diversion
Flow in floodplain	No floodplain	Approximate flow field (90° at inflow boundary)	2D flow field
Morphodynamic results			
Lateral overflow prediction due to deposition	Good	Good	Good
Deposition	Sediment aggradation down-stream good, but no transversal distinction of local deposition	Sediment aggradation down-stream good, but no transversal distinction of local deposition	Good
Relative computing time	Short	Medium	Long

1 The flow in the main channel is not angled at the lateral diversion structure.

main channel. In general, the presented numerical models facilitate transient hydrodynamic simulations of flood events, accounting for discharge reduction due to lateral overflow over the diversion structure. All of the presented model types (1D, 1D–2D coupled and 2D) show the sediment aggradation downstream of the lateral diversion structure, which may increase lateral overflow and thus the required capacity of the retention area or the flood corridor. The side weir discharge coefficient C_M in the 1D and 1D–2D coupled modelling approaches is subject to uncertainty, and good results can be achieved using the simplified approach proposed by Hager (1987). In a 2D model, the coefficient C_M becomes obsolete and the flow in the floodplain or retention area can be simulated in addition to the channel flow. Only 2D models capture local deposition, making them the most suitable option for simulating bed level changes near the diversion structure.

The advantages (green) and disadvantages (red) of the three modelling approaches for simulating lateral diversion structures are listed in Table 4. We recommend designing lateral diversion structures using morphodynamic models. The choice of modelling approach to simulate the lateral overflow, i.e. 1D, 1D–2D coupled or 2D, depends on the model requirements, data availability and objectives.

Box 7: In practice – Ecological flooding of retention areas

Eva Gerke, VAW, ETH Zurich

The goal of ecological flooding is to establish stable, self-sustaining and flood-tolerant populations, i.e. to accustom the flora and fauna to regular flooding (Meurer and Pfarr 2018). In contrast, infrequent flooding with a return period of 30 years or more is not sufficient for the dynamic development of biodiversity in floodplains in retention areas.

A prerequisite for effective ecological flooding is the diversion of water into the retention area at low discharge. This requires a controllable inlet structure, which can be arranged separately from the diversion structure used for flood protection. Free flow of water through the retention area is needed, and stagnant water zones with oxygen depletion should be avoided. Additionally, high flow dynamics are beneficial for erosion and sedimentation processes typical of floodplains. Attention must also be paid to land use. In particular, original floodplains or separated floodplains are suitable. If the retention area is already used for agriculture, ecological flooding makes little sense. However, in the case of mixed use, part of the area can be considered for ecological flooding.

An example of the implementation of ecological flooding is the Altenheim flood retention area along the upper Rhine river in Baden-Württemberg (Germany). The frequency, duration and amount of discharge diverted during an ecological flooding event depend on the current runoff situation in the Rhine river. The status of the restoration of biotic communities in the floodplains is monitored using random samples. Overall, a trend towards both higher biodiversity and a visible dominance of more flood-tolerant species in the frequently flooded areas has been observed (Pfarr 2014).